

Quasiperiodic oscillations in a strong gravitational field around neutron stars testing braneworld models

Andrea Kotrlová, Zdeněk Stuchlík and Gabriel Török

Institute of Physics, Faculty of Philosophy and Science, Silesian University in Opava,
Bezručovo nám. 13, CZ-746 01 Opava, Czech Republic

E-mail: Andrea.Kotrlova@fpf.slu.cz

Abstract. The strong gravitational field of neutron stars in the brany universe could be described by spherically symmetric solutions with a metric in the exterior to the brany stars being of the Reissner–Nordström type containing a brany tidal charge representing the tidal effect of the bulk spacetime onto the star structure. We investigate the role of the tidal charge in orbital models of high-frequency quasiperiodic oscillations (QPOs) observed in neutron star binary systems. We focus on the relativistic precession model. We give the radial profiles of frequencies of the Keplerian (vertical) and radial epicyclic oscillations. We show how the standard relativistic precession model modified by the tidal charge fits the observational data, giving estimates of the allowed values of the tidal charge and the brane tension based on the processes going in the vicinity of neutron stars. We compare the strong field regime restrictions with those given in the weak-field limit of solar system experiments.

PACS numbers: 97.10.Gz, 04.50.Gh, 97.60.Jd, 97.80.Jp

1. Introduction

The string and M-theories describing gravity as higher-dimensional interaction appearing to be effectively 4D at low energies inspired braneworld models with the observable universe being a 3-brane (domain wall) to which the standard non-gravitational matter fields are confined; on the other hand, gravity enters the extra spatial dimensions allowed to be much larger than $l_P \sim 10^{-33}$ cm [1]. Gravity can be localized near the brane even with an infinite size extra dimension with the warped spacetime satisfying the 5D Einstein equations with a negative cosmological constant, as shown by Randall and Sundrum [2]. Consequently, an arbitrary energy-momentum tensor could be allowed on the brane with effective 4D Einstein equations [3].

The Randall–Sundrum model gives standard 4D Einstein equations in the low-energy limit, but significant deviations occur at very high energies, e.g., in the vicinity of compact objects, such as black holes [4] or neutron stars [5]. There are high-energy effects of local origin influencing pressure of matter and non-local effects of “back-reaction” origin arising from the influence of the Weyl curvature of the bulk space on the brane. The combination of the high-energy (local) and bulk stress (non-local) effects alters significantly the matching problems on the brane in comparison with the standard 4D gravity [6], and the stresses induced by the bulk gravity imply that the matching conditions do not have unique solution on the brane [6]. The 5D Weyl tensor is needed as a minimum condition for uniqueness, but no exact 5D solution is known recently [5].

Assuming a spherically symmetric metric induced on the brane, solutions of the effective 4D Einstein equations could be found relatively easily. The vacuum (in both the bulk and brane) solutions represent black holes (naked singularities) of the Reissner–Nordström (RN) type endowed with a brany tidal charge parameter b , describing the bulk tidal stress effect on the black hole structure [4]. In the brany RN metric, the tidal charge b stands instead of the charge parameter Q^2 of the standard RN spacetimes [7]; b can be both positive and negative, but there are indications that $b < 0$ should properly represent the effects of the bulk space Weyl tensor [4, 8, 6].‡

In the case of spherically symmetric neutron stars (or quark stars) simplified by the uniform energy density profile, the local high-energy and non-local bulk graviton stress effects make the matching conditions unambitious, since we do not know the 5D Weyl tensor. Note that the uniform energy density distribution model of neutron stars could, in principle, be used in order to roughly determine the neutron star spacetime structure, since in realistic models with a variety of realistic equations of state, the energy density profile happens to be nearly uniform in most of the neutron star interior [10, 11].

Two different exact exterior solutions related to the uniform density interior are known, both having asymptotically Schwarzschild character [5]. The first one is of the known RN type with the tidal charge and mass parameters being influenced by the

‡ The stationary and axially symmetric vacuum solutions describing rotating black holes (naked singularities) are found to be of the Kerr–Newman type endowed again with the tidal charge reflecting the effect of the bulk stresses [9].

energy density of the star and the brane tension. The second one is more complicated, with metric components being explicitly dependent on the energy density and brane tension [5]. Quite recently, the solution of the RN type was used in the weak-field limit in order to obtain restrictions on the brany parameter and the brane tension from the standard tests on the Mercury perihelion precession, deflection of light near the edge of Sun and the radar echo experiments [12]. Here, we also restrict our investigations to the metric of the RN type in order to obtain an idea of the tidal charge relevance in a strong gravitational field near neutron stars (or black holes) and to find restrictions on the allowed values of the brany parameter. The choice of the RN type of the uniform star brany solutions is supported by a recent study of static exteriors of non-static brany stars showing that spherical non-rotating star solutions admit only Schwarzschild or RN type exterior [13]. Since the junction conditions of the internal and external neutron star spacetimes relate the tidal charge to the brane tension and the energy density (mass and radius) of the neutron star, we can, in principle, also put restrictions on the allowed values of the brane tension [5].

There is a variety of papers related to both weak-field [14] and strong-field [15, 16, 17] optical lensing phenomena in the braneworld black hole spacetimes. The optical phenomena connected to the accretion disc radiation could also reflect in a relevant way the influence of the tidal charge [18, 19]. Here we focus our attention on the strong-field phenomena closely related to the perihelion precession effect discussed in the weak-field limit [12].

High-frequency quasiperiodic oscillations (QPOs) observed in Galactic low-mass binary systems, namely, in both the black hole [20, 21, 22, 23] and neutron star binary systems [24, 25, 26, 27], or in extragalactic black hole sources [28, 29, 30, 31], represent such an interesting phenomenon in the strong field regime enabling estimates of the tidal charge on the basis of orbital models. It is widely accepted that the high-frequency QPOs are related to the orbital motion in the inner part of an accretion disc around a compact object. There are strong indications that some resonant phenomena could be relevant in both black hole systems where twin peak QPOs with fixed frequencies and their ratios are observed [23], and neutron star systems with wide spread of frequencies and their ratios where the twin peak QPOs are cumulated around small number ratios [32, 33]. The hypothetical resonances of the orbital epicyclic oscillations representing plausible models of QPOs were recently studied for brany Kerr black holes [34]. Here, we study these models as related to the brany neutron stars described approximately by the RN spacetimes, i.e., neglecting the effects related to rotation of neutron stars. We focus our attention to the relativistic precession model [35] that fits qualitatively well in the wide spread data given by observations of a variety of neutron star binary systems [24, 25, 26, 27]. However, recently it has been discussed in the case of the atoll source 4U 1636–53 [32, 33, 36] and some other atoll sources [37] that the resonant phenomena should be relevant even in the framework of the relativistic precession (RP) model. We, thus, present a first study of strong-field phenomena for brany neutron stars that could be compared with the weak-field results (perihelion precession, radar echo

delay and light deflection) based on the RN solutions used to describe approximately the spacetime in the vicinity of Sun [12]. In order to obtain rough restrictions on both the brany tidal charge and brane tension, we use an ensemble of typical neutron star atoll sources and the special cases of the Z-sources Sco X-1 and Circinus X-1 that demonstrate a wide variety of QPOs.

In section 2, the effective 4D Einstein equations are presented, and the braneworld neutron star spacetime of the RN type (approximated by the uniform energy density distribution [5]) is briefly described. In section 3, the circular geodesics are discussed. In section 4, frequencies of the orbital epicyclic oscillations are given; their radial profiles are discussed, and the resonance conditions are briefly described for some frequency ratio functions modeling twin peak QPOs. In section 5, the RP model is used to fit data observed in the representative ensemble of neutron star X-ray binaries exhibiting QPOs, and the restrictions on the tidal charge and brane tension are given. In section 6, concluding remarks are presented.

2. Gravitational field equations on the brane and the exterior spacetime to the uniform density configurations

In the 5D warped space models involving a non-compact extra dimension, the gravitational field equations in the bulk can be expressed in the form [3, 4]

$$\tilde{G}_{AB} = \tilde{k}^2[-\tilde{\Lambda}g_{AB} + \delta(\chi)(-\lambda g_{AB} + T_{AB})], \quad (1)$$

where the fundamental 5D Planck mass \tilde{M}_P enters via $\tilde{k}^2 = 8\pi/\tilde{M}_P^3$, λ is the brane tension, and $\tilde{\Lambda}$ is the bulk cosmological constant.

The effective gravitational field equations induced on the brane are determined by the bulk field equation (1), the Gauss–Codazzi equations and the generalized matching Israel conditions with Z_2 symmetry. They can be expressed as modified standard Einstein’s equations containing additional terms reflecting bulk effects onto the brane [3]:

$$G_{\mu\nu} = -\Lambda g_{\mu\nu} + k^2 T_{\mu\nu} + \tilde{k}^2 S_{\mu\nu} - E_{\mu\nu}, \quad (2)$$

where $k^2 = 8\pi/M_P^2$, with M_P being the brany Planck mass. The relations of the energy scales and cosmological constants are given in the form

$$M_P = \sqrt{\frac{3}{4\pi}} \left(\frac{\tilde{M}_P^2}{\sqrt{\lambda}} \right) \tilde{M}_P; \quad \Lambda = \frac{4\pi}{\tilde{M}_P^3} \left[\tilde{\Lambda} + \left(\frac{4\pi}{3\tilde{M}_P^3} \right) \lambda^2 \right]. \quad (3)$$

Requirement of zero cosmological constant on the brane ($\Lambda = 0$) implies the relation

$$\tilde{\Lambda} = -\frac{4\pi\lambda^2}{3\tilde{M}_P^3}. \quad (4)$$

Local bulk effects on the matter are determined by the “squared energy-momentum” tensor $S_{\mu\nu}$ arising from the extrinsic curvature term in the projected Einstein tensor:

$$S_{\mu\nu} = \frac{1}{12} T T_{\mu\nu} - \frac{1}{4} T_\mu^\alpha T_{\nu\alpha} + \frac{1}{24} g_{\mu\nu} (3T^{\alpha\beta} T_{\alpha\beta} - T^2), \quad (5)$$

where $T_{\mu\nu}$ is the energy-momentum tensor on the brane. The non-local bulk effects are given by the tensor $E_{\mu\nu}$, representing the bulk Weyl tensor, \tilde{C}_{ACBD} , projected onto the brane, whereas

$$E_{AB} = \tilde{C}_{ACBD} n^C n^D. \quad (6)$$

There are two known solutions of the effective 4D Einstein equations corresponding to the brany uniform density configurations that could roughly represent the spacetime exterior to neutron (quark) stars [5]. Here, we focus our attention on the solution of the Reissner–Nordström type that is formally identical to the spherically symmetric black hole solution; however, its parameters are related to the brane tension λ and energy density ρ of the internal configuration due to the matching conditions of the internal and external spacetimes. The external spacetime is given in the standard Schwarzschild coordinates by the line element:

$$ds^2 = -A(r)c^2 dt^2 + A^{-1}(r) dr^2 + r^2 d\theta^2 + r^2 \sin^2 \theta d\phi^2, \quad (7)$$

$$A(r) = 1 - \frac{2r_G}{r} + \frac{B}{r^2}; \quad r_G = \frac{GM}{c^2}, \quad (8)$$

where M is the gravitational mass, and B is the brany tidal charge representing the bulk non-local effects on the 4D spacetime structure. The matching conditions imply [5]

$$B = -\frac{3GM}{c^2} R \left(\frac{\rho}{\lambda} \right), \quad (9)$$

$$M = \tilde{M} \left(1 - \frac{\rho}{\lambda} \right), \quad (10)$$

where R is the internal configuration radius, and the effective mass is given by

$$\tilde{M} = 4\pi \int_0^R \rho^{\text{eff}}(r) r^2 dr, \quad (11)$$

with the effective density given by

$$\rho^{\text{eff}} = \rho \left(1 + \frac{\rho}{2\lambda} \right) + \frac{6}{(8\pi G)^2 \lambda} \mathcal{U}. \quad (12)$$

The non-local bulk gravitational effects arising from the bulk Weyl tensor are represented by the “dark energy” density \mathcal{U} . The standard general relativistic equations are regained in the limit of $\lambda^{-1} \rightarrow 0$.

The internal solution puts two important restrictions on the brane tension λ [5]. The first one is general for all uniform stars and reads

$$\lambda \geq \left(\frac{GM/c^2}{R - 2GM/c^2} \right) \rho, \quad (13)$$

implying $R > 2GM/c^2$, i.e., the Schwarzschild radius is still the relevant limit as in general relativity.

The second one represents an upper limit on compactness of the star following from the requirement that pressure must be finite inside the star. It takes the form [5]

$$\frac{GM/c^2}{R} \leq \frac{4}{9} \left[\frac{1 + 5\rho/4\lambda}{(1 + \rho/\lambda)^2} \right] \quad (14)$$

that implies the general relativistic limit $(GM/c^2)/R \leq 4/9$ for $\lambda^{-1} \rightarrow 0$. We can see that the braneworld high-energy corrections reduce the compactness limit of the star and the lowest order correction reads

$$\frac{GM/c^2}{R} \leq \frac{4}{9} \left(1 - \frac{3\rho}{4\lambda} \right). \quad (15)$$

3. Circular geodesics of the external spacetime

Considering vacuum spacetimes, the event horizons of the brany RN metric are determined by the condition $A(r) = 0$. Using geometric units ($c = G = 1$), the radius of the outer event horizon is given by the relation

$$r_+ = M + \sqrt{M^2 - B}. \quad (16)$$

The horizon structure depends on the sign of the tidal charge B . We see that, in contrast to its positive values, the negative tidal charge tends to increase the horizon radius (see, e.g., figure 1).

It is clear that the positive tidal charge acts to weaken the gravitational field, and we have the same horizon structure as in the usual Reissner–Nordström solution. However, new interesting features arise for the negative tidal charge. For $B < 0$, it follows from equation (16) that the horizon radius [4]

$$r_+ > 2M; \quad (17)$$

such a situation is not allowed in the framework of general relativity.

The event horizon does exist provided that $M^2 \geq B$, where the equality corresponds to the extreme case. For $B > M^2$ we obtain a naked singularity spacetime. Clearly, such a situation is impossible for negative values of the brany tidal charge B . Here, we are confronted with another situation, since the vacuum spacetime is limited to $r > R$ and at $r = R$ it has to be matched to the internal uniform density spacetime. Clearly, the radius R must satisfy the compactness condition (14).

Note that values of the brany tidal charge B are not restricted for both positive and negative values; therefore, the external spacetimes with $B > M^2$ (corresponding to the “naked singularity” case) have to be considered too.

In the analysis of the epicyclic frequency profiles, it is useful to relate the profiles to the photon circular geodesic and innermost stable circular geodesic radii (or innermost bound circular geodesic radii in the case of thick discs not considered here), which are relevant in the discussion of properties of the accretion discs and their oscillations. Therefore, we put the limiting radii in an appropriate form.

Introducing the dimensionless radial coordinate

$$x = \frac{r}{r_G} \quad (18)$$

and a dimensionless brany parameter

$$b = \frac{B}{r_G^2}, \quad (19)$$

the metric coefficient takes the form

$$A(x, b) = 1 - \frac{2}{x} + \frac{b}{x^2}. \quad (20)$$

The motion of a test particle with mass m is given by the standard geodesic equation $DU^\mu/d\tau = 0$ and the normalization condition $U_\mu U^\mu = -m^2$. The motion is restricted to the central planes; for one particle the plane can be chosen to be the equatorial plane ($\theta = \pi/2 = \text{const}$). Then, the relevant radial equation of motion takes the form

$$\left(\frac{dx}{d\tau}\right)^2 = E^2 - V_{\text{eff}}^2(x, L, b), \quad (21)$$

where the effective potential

$$V_{\text{eff}}^2(x, L, b) = A(x, b) \left(m^2 + \frac{L^2}{x^2} \right). \quad (22)$$

There are two constants of motion related to the spacetime symmetries: E/m is the specific energy; L/m is the specific angular momentum. The circular geodesic orbits (determined by $\partial V_{\text{eff}}/\partial x = 0$) have the specific energy and the specific angular momentum given by

$$\frac{E}{m} = \frac{x^2 - 2x + b}{x(x^2 - 3x + 2b)^{1/2}}, \quad (23)$$

$$\frac{L}{m} = \pm \frac{x\sqrt{x-b}}{(x^2 - 3x + 2b)^{1/2}}. \quad (24)$$

From equations (23) and (24) we can see that the circular orbits can exist from infinity down to the radius of the limiting circular photon orbit, determined by the condition

$$x^2 - 3x + 2b = 0, \quad (25)$$

where $E/m \rightarrow \infty$ and $L/m \rightarrow \pm\infty$, but the impact parameter $I = L/E$ remains finite. For “naked singularity” RN spacetimes, the restriction

$$x \geq b \quad (26)$$

can be relevant.

The radius of the marginally bound orbits with $E^2 = m^2$ is given by the largest root of the equation

$$x(4x - x^2 - 4b) + b^2 = 0, \quad (27)$$

while the stable circular orbits are restricted by the condition

$$x(6x - x^2 - 9b) + 4b^2 \leq 0. \quad (28)$$

The outer event horizon $x_{\text{h}}(b)$ is implicitly determined by the relation

$$b = b_{\text{h}}(x) \equiv x(2 - x), \quad (29)$$

the radius of the photon circular orbit $x_{\text{ph}}(b)$ is given by

$$b = b_{\text{ph}}(x) \equiv \frac{x}{2}(3 - x), \quad (30)$$

the radius of the marginally bound orbit $x_{\text{mb}}(b)$ is given by

$$b = b_{\text{mb}}(x) \equiv x (2 \mp \sqrt{x}), \quad (31)$$

and the radius of the marginally stable orbit $x_{\text{ms}}(b)$ is given by

$$b = b_{\text{ms}}(x) \equiv \frac{x}{8} (9 \mp \sqrt{16x - 15}). \quad (32)$$

The upper sign in (31) and (32) is relevant for the black hole spacetimes in the region above the outer horizon, while both signs are relevant for the naked singularity spacetimes.

Now, we have to put the limits on the applicability of the vacuum spacetime using the limit condition on the compactness of the uniform internal configuration given by the relation (14). We shall give the limits in terms of the dimensionless brany tidal charge b that can be expressed in the form

$$b = -3 \frac{R}{r_{\text{G}}} \left(\frac{\rho}{\lambda} \right) = -3X \left(\frac{\rho}{\lambda} \right). \quad (33)$$

Clearly, negative (positive) values of b correspond to positive (negative) values of the brany tension λ .

The compactness relation (14) then reads

$$4 - \left(9 + \frac{5}{3}b \right) \left(\frac{r_{\text{G}}}{R} \right) + 6b \left(\frac{r_{\text{G}}}{R} \right)^2 - b^2 \left(\frac{r_{\text{G}}}{R} \right)^3 \geq 0, \quad (34)$$

and in the linear form

$$\left(\frac{r_{\text{G}}}{R} \right) \leq \frac{4}{9 - b}. \quad (35)$$

The equality in relation (34) determines the critical radius R_{C} representing the limit on the radius of neutron stars. We have to restrict our studies to the region $r > R_{\text{C}}$. The radii $X_{\text{C}} = R_{\text{C}}/r_{\text{G}}$ are illustrated in figure 1, and are given (in an implicit form) by the relation

$$b = b_{\text{C}}(x) \equiv \frac{1}{6} (18x - 5x^2 \mp x^{3/2} \sqrt{25x - 36}). \quad (36)$$

The functions $b_{\text{h}}(x)$, $b_{\text{ph}}(x)$, $b_{\text{mb}}(x)$, $b_{\text{ms}}(x)$ and $b_{\text{C}}(x)$ are illustrated in figure 1. It is evident that the positive tidal charge will play the same role in its effect on the circular orbits as the electric charge in the Reissner–Nordström spacetime – the radius of the circular photon orbit, as well as the radii of the innermost bound and the innermost stable circular orbits shift inwards as the positive tidal charge increases. For the negative tidal charge the limiting photon orbit, the innermost bound and the innermost stable circular orbits shift outwards as the absolute value of b increases [4, 9]. Of special interest is the behaviour of $b_{\text{C}}(x)$ putting limits on validity of the internal uniform density configuration. For $b = 0$, the limit is $X_{\text{C}} = 9/4$, and it falls with $b > 0$ growing up to $b \doteq 2.6$, where it starts to grow again. On the other hand, for $b < 0$ the critical radius X_{C} slowly grows with b descending to higher negative values, but for $b = -1.5$, there is $X_{\text{C}} = x_{\text{h}}$, and the function $b_{\text{C}}(x)$ loses its relevance leaving $X > x_{\text{h}}$ as the only basic restriction on the surface radius of the neutron star.

The function $b_h(x)$ has a local maximum at $x = 1$ where $b = 1$, corresponding to the extreme case. This local maximum coincides with the local minimum of the function $b_{ms}(x)$ at $x = 1$. The function $b_{ph}(x)$ has a local maximum at $x = 3/2$ for $b = 9/8$ corresponding to the naked singularity spacetimes. The local maximum of the function $b_{mb}(x)$ is located at $x = 16/9$ for $b = 32/27$; the function $b_{ms}(x)$ has a local maximum situated at $x = 5/2$ for $b = 5/4$ (this local maxima appear again only for naked singularities); the function $b_C(x)$ crosses $b_h(x)$ at $b = -1.5$ (see figure 1). Clearly, due to the compactness limit $b_C(x)$, the photon circular orbits are relevant in the spacetimes with $b \leq 1.017$ only. Further, we immediately see that for $b > 0$, the marginally stable orbits are well defined in the black hole type spacetimes ($b \leq 1$) and in naked singularity type spacetimes with $b \leq 5/4$ and $b > 9/4$. In the spacetimes with $5/4 < b \leq 9/4$, the stable orbits can be located at all $x \geq X_C$, since $x_{ms} < X_C$ (and $x_{ms} = X_C$ for $b = 9/4$) in such vacuum RN spacetimes.

4. Epicyclic oscillations of Keplerian motion

It is well known that for oscillations of both thin Keplerian [38, 39] and toroidal discs [40] around neutron stars (black holes) the orbital Keplerian frequency ν_K and the related radial and vertical epicyclic frequencies ν_r and ν_θ of geodetical quasicircular motion are relevant and observable directly or through some combinational frequencies [23, 41, 42, 43]. Of course, for extended tori, the eigenfrequencies of their oscillations are shifted from the epicyclic frequencies in dependence on the thickness of the torus [44, 45]. Similarly, due to non-linear resonant phenomena, the oscillatory eigenfrequencies could be shifted from the values corresponding to the resonant geodetical epicyclic frequencies in dependence on the oscillatory amplitude [46, 47]. It is expected that shift of this kind is observed in neutron star systems [48, 49], while in microquasars, i.e., binary black hole systems, the observed frequency scatter is negligible and the geodetical epicyclic frequencies should be relevant.

In the case of the external braneworld neutron star spacetime of the RN type with the brany tidal charge b , the formulae of the test particle geodetical circular motion and its epicyclic oscillations, obtained in [50], could be directly applied (putting $a = 0$ and $Q^2 = b$). We can write the following relations for the orbital and epicyclic frequencies:

$$\nu_K = \frac{1}{2\pi} \left(\frac{GM}{r_G^3} \right)^{1/2} \frac{1}{x^{3/2}} \left(1 - \frac{b}{x} \right)^{1/2} = \frac{1}{2\pi} \frac{c^3}{GM} \frac{1}{x^{3/2}} \left(1 - \frac{b}{x} \right)^{1/2}, \quad (37)$$

$$\nu_\theta^2 = \alpha_\theta \nu_K^2, \quad (38)$$

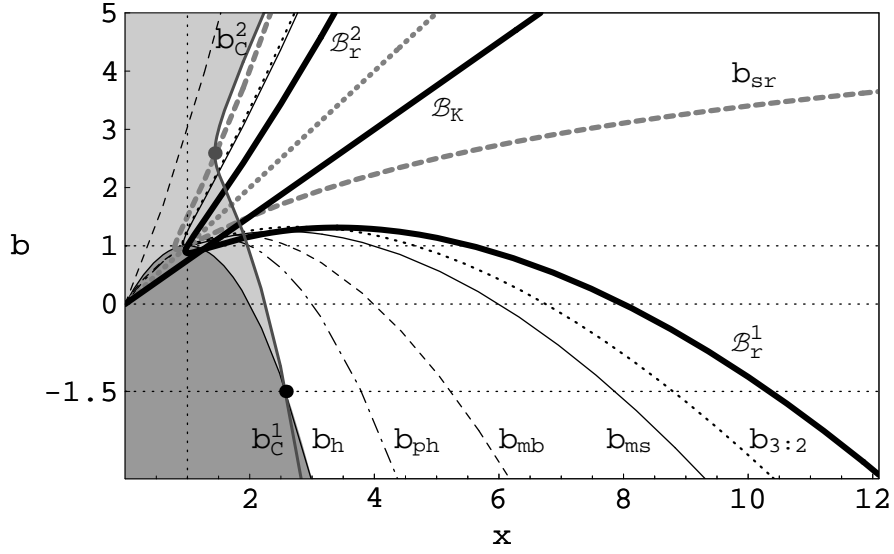
$$\nu_r^2 = \alpha_r \nu_K^2, \quad (39)$$

where the dimensionless quantities determining the epicyclic frequencies are given by

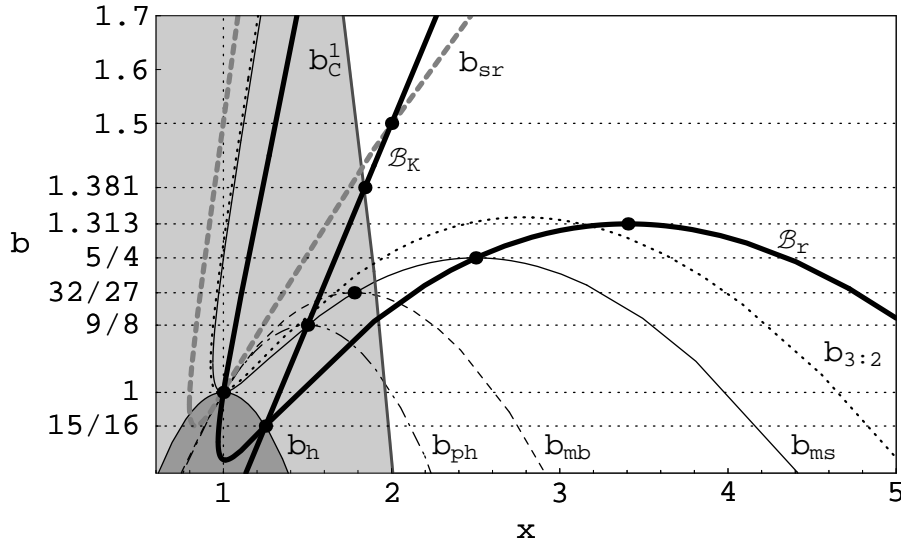
$$\alpha_\theta = 1, \quad (40)$$

$$\alpha_r = \left(1 - \frac{b}{x} \right)^{-1} \left(1 - \frac{6}{x} + \frac{9b}{x^2} - \frac{4b^2}{x^3} \right), \quad (41)$$

so that $\nu_K(x, b) = \nu_\theta(x, b)$ due to the spherical symmetry of the spacetime.



(a)



(b)

Figure 1. (a) The functions b_h (black solid line), b_{ph} (dashed-dotted line), b_{mb} (dashed line) and b_{ms} (thin black solid line) that implicitly determine the radius of the outer event horizon, the limiting photon orbit and the marginally bound and marginally stable circular orbits of a braneworld RN type spacetime. The grey solid line represents the function b_C implicitly determining the critical radius X_C of neutron stars. The thick black solid lines represent the functions $\mathcal{B}_K(x = \mathcal{X}_K)$ and $\mathcal{B}_R^k(x = \mathcal{X}_r)$, implicitly determining the locations \mathcal{X}_K and \mathcal{X}_r of the Keplerian and radial epicyclic frequency local extrema. Thick grey dotted line represents the function $b = x$ determining the other limit on the reality of circular orbits. The function b_{sr} that implicitly determines the strong resonant radius x_{sr} , where $\nu_K(x, b) = \nu_r(x, b)$ ($\alpha_r(x, b) = 1$) is denoted by thick grey dashed line. The function $b_{3:2}$ (black dotted line) represents the radii, where the relativistic precession resonance $\nu_K : (\nu_K - \nu_r) = 3 : 2$ occurs. (b) The detailed figure introduces the relevant values of the brany tidal charge, separating the external spacetimes of different properties.

In the field of brany RN black holes (neutron stars) with $b \leq 1$, there is (see figure 2)

$$\nu_K(x, b) > \nu_r(x, b). \quad (42)$$

However, this statement is not generally correct in the case of brany RN naked singularities (neutron stars) with $b > 1$. For $b > 1.42$, the case $\nu_K(x, b) < \nu_r(x, b)$ is even possible in some region of the external (vacuum) spacetime.

Now we can discuss the behaviour of the fundamental orbital frequencies for Keplerian motion in the field of both brany RN black hole and brany RN naked singularity spacetimes, i.e., we consider external neutron star spacetimes with tidal charge $b \leq 1$ and $b > 1$. (Note that $b < 0$ always corresponds to the black hole spacetime behaviour.)

We express the frequency as ν [Hz] $10 M_\odot/M$ in every quantitative plot of frequency dependence on radial coordinate x , i.e., displayed value is the frequency relevant for a central object with a mass of $10 M_\odot$, which could be simply rescaled for another mass just by dividing the displayed value by the respective mass in units of ten solar masses.

4.1. Properties of the Keplerian and radial epicyclic frequency

First, it is important to find the range of relevance for the functions $\nu_K(x, b)$ and $\nu_r(x, b)$ above the critical radius R_C of neutron stars. For completeness we consider their behaviour above the event horizon x_h for black holes (neutron stars), and above the ring singularity located at $x = 0$ for naked singularities; recall that in the external spacetimes with $b < -1.5$, the restriction by $x > X_C(b)$ is irrelevant, but the horizon condition $x > x_h(b)$ keeps its relevance.

The circular geodesics can exist for $x > x_{ph}(b)$, where $x_{ph}(b)$ is implicitly determined by the equation (25). Stable circular geodesics, relevant for the Keplerian, thin accretion discs, exist for $x > x_{ms}(b)$, where $x_{ms}(b)$ is determined (in an implicit form) by the relation (28), which coincides with the condition

$$\alpha_r(x, b) = 0. \quad (43)$$

For toroidal, thick accretion discs the unstable circular geodesics can be relevant in the range $x_{mb} \leq x_{in} < x < x_{ms}$, being stabilized by pressure gradients in the tori [51, 52]. The radius of the marginally bound circular geodesic x_{mb} , implicitly determined by the equation (27), is the lower limit for the inner edge of thick discs [53, 54].

Clearly, the Keplerian orbital frequency is well defined up to $x = x_{ph}$. However, ν_r is well defined, if $\alpha_r \geq 0$, i.e., at $x \geq x_{ms}$, and $\nu_r = 0$ at x_{ms} . From figure 2, we can conclude that not only the radial epicyclic frequency but even the Keplerian frequency can have a maximum located above the outer event black hole horizon. In the following subsection, we will discuss whether the maximum of $\nu_K(x, b)$ could be located above the marginally stable or the limiting photon circular orbit.

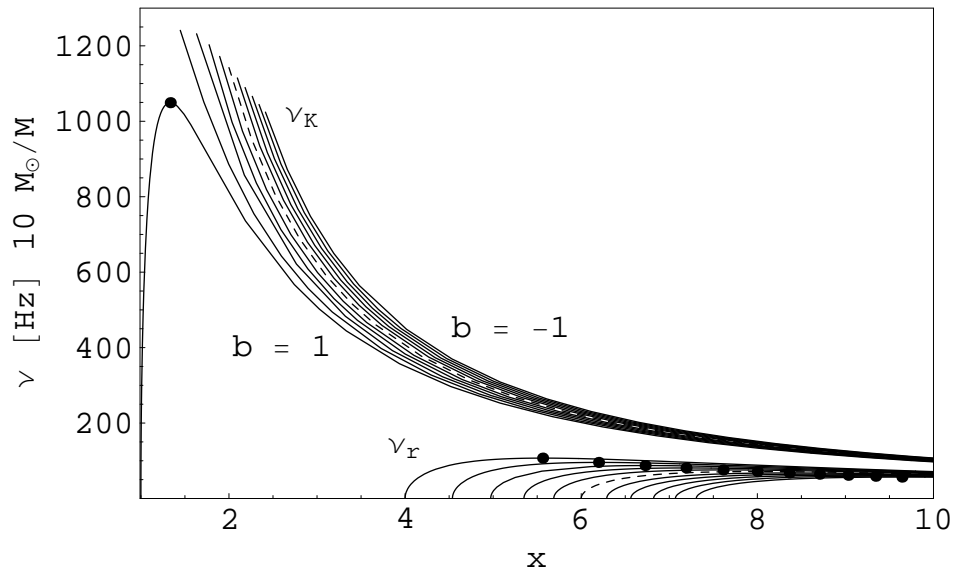


Figure 2. The behaviour of the Keplerian frequency ν_K and radial epicyclic frequency ν_r in the field of braneworld RN black hole (neutron star) spacetimes with various values of the tidal charge parameter b . The curves are spaced by 0.2 in b , and they are plotted from the outer event black hole horizon x_h . The dashed lines represent Schwarzschild spacetime with zero tidal charge.

4.1.1. Local extrema of the Keplerian frequency. We denote by \mathcal{X}_K the local extrema of the Keplerian frequency $\nu_K(x, b)$ given by the condition

$$\frac{\partial \nu_K}{\partial x} = 0. \quad (44)$$

From (37), we find that after introducing ' as d/dx the corresponding derivative is given by

$$\nu'_K = \frac{1}{2\pi} \sqrt{\frac{GM}{r_G^3}} \frac{4b - 3x}{2x^3 \sqrt{x - b}} = \frac{4b - 3x}{2x(x - b)} \nu_K, \quad (45)$$

and relation (44) implies that the Keplerian frequency has a local extremum located at

$$\mathcal{X}_K = \frac{4}{3}b. \quad (46)$$

The second derivative at $x = \mathcal{X}_K$,

$$\nu''_K = -\frac{1}{2\pi} \sqrt{\frac{GM}{r_G^3}} \frac{81\sqrt{3}}{128 b^3 \sqrt{b}}, \quad (47)$$

is always negative; thus, the Keplerian frequency has a local maximum at $x = \mathcal{X}_K$.

For $b = 15/16$, the maximum of the Keplerian frequency radial profile is situated exactly at the radius coinciding with the radius of the outer event horizon $\mathcal{X}_K = x_h = 5/4$ (see figures 1(b) and 3). For $b = 9/8$, the maximum of the Keplerian frequency is located at the circular photon orbit $\mathcal{X}_K = x_{ph} = 3/2$ (this case corresponds to the naked singularity spacetime).

We can conclude that for brany parameter from the interval

$$15/16 < b < 9/8 \quad (48)$$

the Keplerian frequency radial profile has its maximum located between the outer event horizon and the circular photon orbit:

$$x_h < \mathcal{X}_K < x_{\text{ph}}, \quad (49)$$

i.e., it is physically irrelevant there.

Generally, the maximum of the Keplerian frequency is physically irrelevant for all the brany RN neutron stars (of the black hole type with $b \leq 1$), since it could never be located above the circular photon orbit x_{ph} (and the marginally stable orbit x_{ms}). For spacetimes with $b \leq 1$, the Keplerian frequency is a monotonically decreasing function of radius in astrophysically relevant radii above the photon orbit, $x > x_{\text{ph}}$. The situation is clearly illustrated in figure 1(b). For the RN naked singularity type spacetimes with $b < 1.381$ the extrema of ν_K must be hidden under the neutron star surface. The local extrema of ν_K can appear in the external spacetime to the internal uniform density configuration for $b > 1.381$ (see also figure 3).

4.1.2. Local extrema of the radial epicyclic frequency. The local extrema of the radial epicyclic frequency \mathcal{X}_r are given by the condition

$$\frac{\partial \nu_r}{\partial x} = 0. \quad (50)$$

Using (39), the derivative reads

$$\nu'_r = \sqrt{\alpha_r} \left(\nu'_K + \frac{\alpha'_r}{2\alpha_r} \nu_K \right), \quad (51)$$

$$\alpha'_r = -\frac{8b}{x^3} + \frac{5}{x^2} + \frac{1-x}{(x-b)^2} + \frac{1}{x-b}, \quad (52)$$

where ν'_K is given by (45). Relations (50) and (51) imply the condition determining extrema $\mathcal{X}_r(b)$ of the radial epicyclic frequency profile:

$$\alpha'_r = -\frac{2\nu'_K}{\nu_K} \alpha_r(x, b). \quad (53)$$

In figure 1, we show curves $\mathcal{B}_r^k(x = \mathcal{X}_r)$, $k \in \{1, 2\}$, implicitly determined by relation (53); index k denotes different branches of the solution of (53):

$$\mathcal{B}_r^k = \frac{x}{16} \left(15 \mp \sqrt{32x - 31} \right). \quad (54)$$

For all possible values of the brany parameter $b \leq 1$, the radial epicyclic frequency ν_r has one local maximum for braneworld RN neutron stars (black holes) that is always located above the marginally stable orbit x_{ms} (see figure 1).

In the case of RN neutron stars with $b > 1$ (naked singularity type spacetimes), the situation is complicated, and the discussion can be separated into four parts according to the parameter b (see figures 1(b) and 3):

(a) $1 < b \leq 5/4$.

The radial epicyclic frequency ν_r has one local maximum as usual in RN spacetimes.

(b) $5/4 < b < b_m \doteq 1.313$.

The radial epicyclic frequency ν_r has one local maximum and one local minimum.

(c) $b_m \leq b \leq b_c \doteq 1.381$.

The radial epicyclic frequency ν_r has no local extrema (for all $b \geq b_m$) since the condition $x > b$ has to be satisfied, and for these values of b there is $\mathcal{X}_r < x = b$.

(d) $b > b_c$.

The maximum of the Keplerian frequency profile could be relevant, since it can appear outside the internal uniform density configuration given by $b_C(x)$.

We can summarize that in braneworld RN spacetimes:

- the Keplerian frequency is a monotonically decreasing function of radius for the whole range of the brany tidal charge parameter b in astrophysically relevant radii above the photon circular orbit (or the neutron star surface); an exception exists at spacetimes with $b > 1.381$, where the photon circular orbit is not defined.
- the radial epicyclic frequency has a local maximum for RN black hole type spacetimes with $b \leq 1$, and vanishes at the innermost stable circular geodesic;
- for RN naked singularity type spacetimes the behaviour of the radial frequency is different; a detailed analysis shows that the radial epicyclic frequency can have one local maximum for $1 < b \leq 5/4$, two local extrema for $5/4 < b < 1.313$ or no local extrema for $b \geq 1.313$.

4.2. Orbital models of QPOs

A number of low-mass X-ray binaries containing a neutron star show quasiperiodic oscillations (QPOs) in their X-ray flux, i.e., peaks in the Fourier variability power density spectra (PDS). Frequencies of some QPOs are in the kHz range corresponding to frequencies of the orbital motion close to the central neutron star. Such so-called high-frequency (kHz) QPOs span large frequency range of 200 – 1400 Hz. The two distinct modes following their own correlation between frequency and properties (amplitude and quality factor) of the peak are observed in this range (see, e.g., [21, 24, 25, 26, 55, 56]). They are called lower and upper QPO because the frequencies of upper QPO, ν_U , is higher than the frequency of the lower QPO, ν_L , when both modes are detected simultaneously; we call them twin peak QPOs in such situations [57, 36, 33, 58]. It was shown that the twin peak QPOs are clustered around frequencies corresponding to the frequency ratio of small integers [32, 33]. In some atoll sources, namely 4U 1636–53 and 4U 1728, the frequency ratios are clustered around 3:2 and 5:4, in others (4U 1608 and 4U 0614) they cluster around 3:2 only, and in 4U 1820 and 4U 1735 they cluster around ratio 4:3 [37]. In the best known Z-source Sco X-1 the frequency ratios cluster around 3:2 and 5:4 [59] and in the exceptional Z-source Circinus X-1, the frequency ratio is clustered around 3:1 at relatively low frequencies ~ 100 Hz [60].

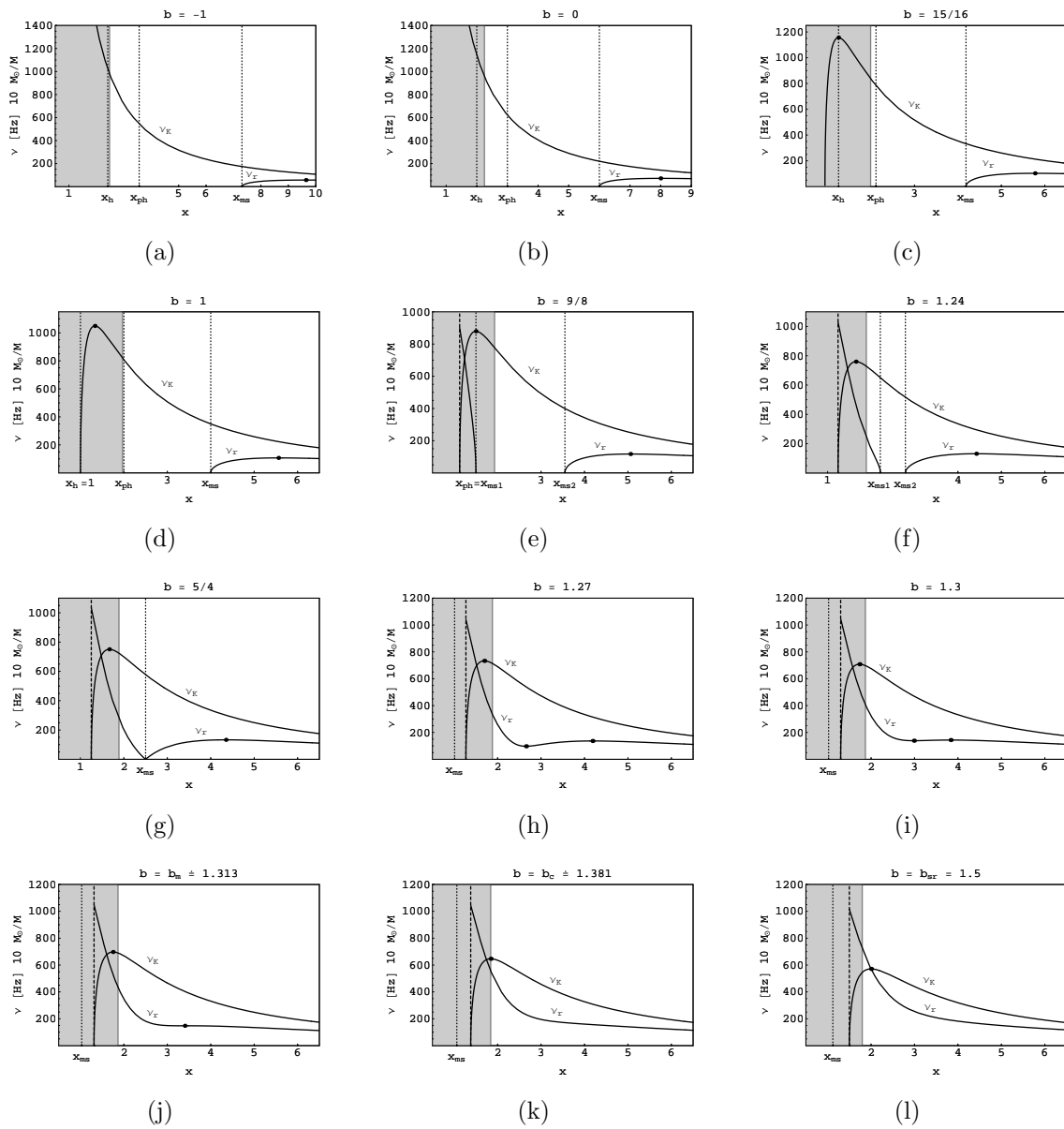


Figure 3. The Keplerian and radial epicyclic frequency profiles for some representative values of the brany parameter b in braneworld RN black hole (neutron star) (a)–(c), the extreme braneworld RN black hole case (d), RN naked singularity spacetimes (e)–(l). The radius of the outer event horizon x_h , the limiting photon orbit x_{ph} and the marginally stable x_{ms} circular orbits are denoted by a dotted vertical line (if these orbits exist at the given spacetime). Note that the condition $x > b$ has to be satisfied, the dashed line in (e)–(l) represents the radius where $x = b$. The grey solid line denotes the critical radius X_C representing the limit on the radius of neutron stars. So the grey area is astrophysically irrelevant. (l) is the special case with $\nu_K = \nu_r$ at $x = \mathcal{X}_K = 2$ for $b = b_{sr} = 1.5$.

Several models have been outlined to explain observational data of the neutron star kHz QPOs assuming that their origin is related to orbital motion near the inner edge of accretion discs around the neutron stars. The RP model of Stella and Vietri [35] introduces the QPOs representing a direct manifestation of modes of a relativistic epicyclic motion of radiating blobs in the innermost parts of the accretion disc. In this model, the upper and lower frequencies are identified in the following way:

$$\nu_U = \nu_K, \quad \nu_L = \nu_K - \nu_r. \quad (55)$$

The resonance model introduced by Abramowicz and Kluźniak [61, 62] (and earlier in other connections by Aliev and Galtsov [50]) assumes a non-linear resonance (forced or parametric) of accretion disc oscillations with vertical and radial epicyclic frequencies ν_θ and ν_r . However, in spherically symmetric spacetimes assumed here $\nu_\theta = \nu_K$, and we identify

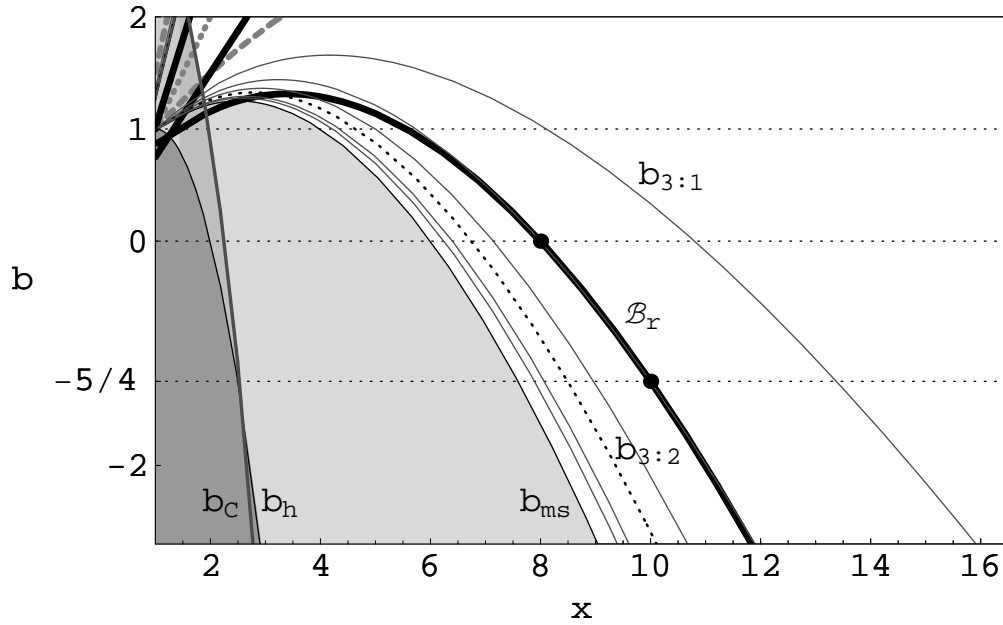
$$\nu_U = \nu_K, \quad \nu_L = \nu_r. \quad (56)$$

The observed frequency ratio ν_U/ν_L decreases with increasing frequencies as $x \rightarrow x_{\text{ms}}$, but ν_K/ν_r increases as $x \rightarrow x_{\text{ms}}$ (see [58] for details). On the other hand, frequency relations implied by the RP model yield a trend, which is in good accord with observation. In other words, frequency relation of the RP model satisfies in a natural way the general tendency of twin peak kHz QPOs as the ratio of $\nu_K : (\nu_K - \nu_r)$ decreases with increasing frequencies ν_K and $\nu_K - \nu_r$ for x approaching the inner edge of the disc at $x = x_{\text{ms}}$, where $\nu_r \rightarrow 0$ and $\nu_K : (\nu_K - \nu_r) \rightarrow 1$. The clustering of the observational data could then be explained by non-linear resonant phenomena between the Keplerian and periastron oscillatory motion in the framework of the multiresonant model [58, 43]. Note, however, that this frequency relation can coincide with those implied under consideration of a forced resonance between the epicyclic frequencies with observed higher eigenfrequency $\nu_U = \nu_K = \nu_\theta$ and lower combinational frequency $\nu_L = \nu_K - \nu_r$. In the spherically symmetric spacetimes, they coincide with radial $m = 1$ and vertical $m = 2$ disc oscillation modes. Here, we focus for simplicity on the RP model.

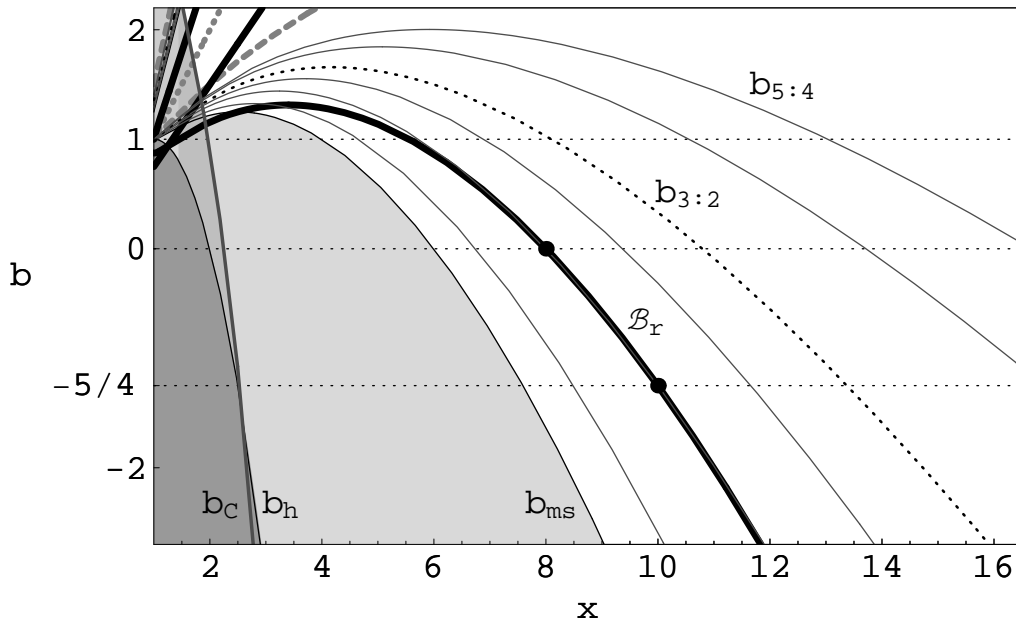
4.3. Resonance radii

Radial profiles of the Keplerian and radial epicyclic frequency in the external spacetimes of the black hole type ($b \leq 1$) enable us to find the observed resonant points (3:2, 4:3, 5:4) and relations for the resonant radii in the framework of both the relativistic precession model frequency relations $\nu_K : (\nu_K - \nu_r)$ and the epicyclic frequency relations $\nu_K : \nu_r$. The same relations hold in the case of external spacetimes of the naked singularity type with $1 < b \leq 5/4$, where the behaviour of the Keplerian and radial epicyclic frequencies is the same as in the black hole type spacetimes. §

§ We do not consider the internal branch of stable orbits since it is too close to the limit given by b_C .



(a)



(b)

Figure 4. The resonant radii for ratios of small integers for the RP model $\nu_K : (\nu_K - \nu_r)$ (a) and for the model of direct resonances $\nu_K : \nu_r$ (b). The grey lines represent the frequency ratios $\nu_U : \nu_L = 3:1, 2:1, 5:3, 3:2$ (dotted line), $4:3$ and $5:4$ subsequently right to left in (a), left to right in (b). For $b = 0$ and $b = -5/4$ the resonance radius where $\nu_U : \nu_L = 2:1$ coincides with the radius of the radial epicyclic frequency local maximum (at $x = 8$ for $b = 0$, at $x = 10$ for $b = -5/4$).

The resonant radii $x_{n:m}$, where the frequency ratio $\nu_K : (\nu_K - \nu_r)$ given by the RP model takes the value $n:m = p$, are implicitly given by the condition

$$b = b^{K/(K-r)}(x, p) \equiv b_{\text{RP}}(x, p) \\ \equiv \frac{(p-1)^2 x^2 + 9p^2 x \mp x \sqrt{x^2 (p-1)^4 + 2p^2 x (9p^2 - 2p + 1) - 15p^4}}{8p^2}. \quad (57)$$

For the model of direct resonances of the epicyclic frequencies we arrive at the relation

$$b = b^{K/r}(x, p) \equiv \frac{x}{8p^2} \left[9p^2 + x \mp \sqrt{x^2 + 2p^2 x + p^4 (16x - 15)} \right]. \quad (58)$$

These models are valid at $x > x_{\text{ms}}$, but their behaviour is inverse as $x \rightarrow x_{\text{ms}}$, since $\nu_K : (\nu_K - \nu_r) \rightarrow 1$ there, while $\nu_K : \nu_r$ diverges there since $\nu_r(x = x_{\text{ms}}) = 0$.

The resonant radii for ratios of small integers allowing for efficient resonant phenomena [46] are given in figure 4. Note that $b_{3:2}^{K/(K-r)}(x) = b_{3:1}^{K/r}(x)$, $b_{2:1}^{K/(K-r)}(x) = b_{2:1}^{K/r}(x)$, $b_{3:1}^{K/(K-r)}(x) = b_{3:2}^{K/r}(x)$. We stress that to model the data of twin peak QPOs in neutron star systems, we can use the RP model, but the direct epicyclic frequency model gives trends just opposite to what is observed.

Using the RP model, we can conclude that the resonant points are located in the region between the marginally stable orbit and the local extremum of the epicyclic frequency, i.e., in the innermost part of the accretion disc. The frequency ratios $\sim 3:1$, observed in the Z-source Circinus X-1 [60] could still be explained in the framework of the RP model, but the resonant points must be located above the maximum of the radial epicyclic frequency. The fitting of the observational data will be discussed in the following section, but for our rough estimates we shall concentrate on the behaviour of the frequency-frequency relations, postponing the detailed studies of the resonant phenomena in individual sources to future studies.

4.3.1. Strong resonance radii. Here, we would like to mention some special resonance conditions that could be realized in the RN spacetimes of the naked singularity type.

For RN naked singularity spacetime with $b > 1.42$, the Keplerian and radial epicyclic frequencies could be equal at a specific radius (see figure 3). The condition $\nu_K(x, b) = \nu_r(x, b)$ implies the relation

$$b = b_{\text{sr}}(x) \equiv \frac{x}{8} \left(9 + x \mp \sqrt{x(x+18) - 15} \right) \quad (59)$$

determining in an implicit way the strong resonant radii, where the resonance between the oscillations with Keplerian and radial epicyclic frequencies could be strongest, and the frequency scatter allowed for the resonance is largest. The function $b_{\text{sr}}(x)$ is illustrated in figure 1. Note, however, that the above relation is not relevant in case of neutron star systems.

5. QPOs and RP model testing the braneworld models

We have summarized the twin peak QPOs data for the atoll sources and Z-sources Sco X-1 and Circinus X-1 in figure 5 using the data accumulated in [25]. Clearly, there is

a general tendency in the $\nu_U - \nu_L$ frequency relations that can be immediately deduced from the observational data: ν_U/ν_L decreases with ν_L (ν_U) increasing as stressed in the previous section.

We shall use the most frequent RP model in order to obtain rough restrictions on the allowed values of the tidal charge (and brane tension) related to neutron star systems giving the observational data demonstrated in figure 5.

Assuming that the trend observed in the frequency relations passing through the clusters of the neutron star twin peak kHz QPOs is related to the modes of the RP model, we make two kinds of fitting the data by the brany neutron star models. From these fittings we deduce rough constraints to the tidal charge and brane tension related to the neutron star systems generating the observed data.

First, we assume negative values of the brany tidal charge (and positive brane tension $\lambda > 0$) and consider any RP model with values of $b < 0$ touching any observational point. Thus, we exclude the values of $b < 0$ that correspond to the RP frequency relations located outside the observational data (see figure 5). The results are characterized by $M = 1.6 M_\odot$ and $b \in (-2.8, 0)$ (see figure 5(a)). Assuming the canonical neutron star mass $M = 1.4 M_\odot$, we obtain the acceptable interval of tidal charge $b \in (-3.6, 0)$ as demonstrated in figure 5(b).

Second, we allow both positive and negative values of b (and brane tension λ). Such a case we represent by an estimate done in a symmetric way, i.e., we find such a neutron star mass that the observational data are scanned for this mass parameter by RP fit relations with brany tidal charge of the same size in both positive and negative values; we have found $M = 2 M_\odot$ and $b \in (-1.2, +1.2)$ as demonstrated in figure 6.||

The presented results are used to obtain estimates on restrictions of the tidal charge B using the relation

$$|B| < |B_{(i)}| = |b_{(i)}| \left(\frac{GM_{(i)}}{c^2} \right)^2. \quad (60)$$

We then obtain the following restrictions:

- (a) Assuming negative tidal charge with $|b_{(1)}| = 2.8$ and $M_{(1)} = 1.6 M_\odot$, we obtain

$$|B| < |B_{(1)}| = 1.562 \times 10^{11} \text{ cm}^2, \quad (61)$$

while the canonical mass $M_{(2)} = 1.4 M_\odot$ and $|b_{(2)}| = 3.6$ yield

$$|B| < |B_{(2)}| = 1.537 \times 10^{11} \text{ cm}^2. \quad (62)$$

- (b) Allowing both positive and negative values of the tidal charge, we obtain for $M_{(3)} = 2 M_\odot$ and $|b_{(3)}| = 1.2$ the estimate

$$|B| < |B_{(3)}| = 1.046 \times 10^{11} \text{ cm}^2 \quad (63)$$

|| Note that the range of $b < 5/4$ enables us to limit our consideration to the RN naked singularity type spacetimes with the same behaviour of the Keplerian and radial epicyclic frequencies as in the black hole spacetimes; for example, the strong resonance radii are irrelevant.

that is naturally lower in comparison with the previous two cases because of the scatter of b into both positive and negative values that reduces the magnitude of the dimensionless tidal charge by a factor of ~ 1.5 .

The brane tension can be estimated using the relation (9), which yields

$$|\lambda| > |\lambda_{(i)}| = \frac{3GM_{(i)} R_{(i)}\rho_{(i)}}{c^2 B_{(i)}} \quad (64)$$

that can be transformed to the relation

$$|\lambda| > |\lambda_{(i)}| = \frac{3\rho_{(i)} R_{(i)}}{|b_{(i)}| r_G} = \frac{3\rho_{(i)}}{|b_{(i)}|} X_{(i)}. \quad (65)$$

Using the limit on compactness of the uniform configuration $R/r_G > R_C/r_G$, where $R_C(b)/r_G = X_C(b)$ is implicitly given as a function of b by relation (36), we arrive at the general estimate on the brane tension:

$$|\lambda| > |\lambda_{(i)}| = \frac{3\rho_{(i)} R_C(b_{(i)})}{|b_{(i)}| r_G} = \frac{3\rho_{(i)}}{|b_{(i)}|} X_C(b_{(i)}). \quad (66)$$

For the canonical values of the neutron stars, namely $M = 1.4 M_\odot$, $R = 10$ km and $\rho \sim 6.6 \times 10^{14}$ g/cm³, we find

$$|\lambda| > |\lambda_{\text{can}}| = 2.7 \times 10^{15} \text{ g/cm}^3. \quad (67)$$

In order to make a more precise restriction of λ , we have to estimate the dimensionless surface radius X of the configuration for given $b_{(i)}$ and $M_{(i)}$. For $b_{(i)} > -1.5$, the estimate should be related to $b_C(x)$, for $b_{(i)} < -1.5$ we have to use $b_h(x)$.

We find

$$|\lambda| > |\lambda_{(i)}| = \frac{3}{|b_{(i)}|} \left(\frac{M_\odot}{M_{(i)}} \right)^2 \left(\frac{1}{X_{(i)}} \right)^2 1.477 \times 10^{17} \text{ g/cm}^3. \quad (68)$$

For $M_{(1)} = 1.6 M_\odot$, $|b_{(1)}| = 2.8$ and choosing $X_{(1)} = 4$, we find

$$|\lambda_1| = 3.9 \times 10^{15} \text{ g/cm}^3, \quad (69)$$

which is comparable to our simple canonical estimate (67). For $M_{(3)} = 2 M_\odot$, $|b_{(3)}| = 1.2$ and choosing $X_{(3)} = 3$, we find

$$|\lambda_3| = 1 \times 10^{16} \text{ g/cm}^3. \quad (70)$$

This estimate exceeds the canonical one by a factor of ~ 3.7 because of the lowering of the dimensionless tidal charge limit.

6. Conclusions

Using the RP model of kHz QPOs observed in neutron star X-ray binaries modified by the hypothetical tidal charge of the neutron stars as implied by the braneworld uniform star model, we are able to put rough restriction on the tidal charge magnitude and brane tension magnitude related to the considered group of atoll sources and some Z-sources. This is the first attempt at an estimate coming from the consideration of effects in the extremely strong gravitational fields.

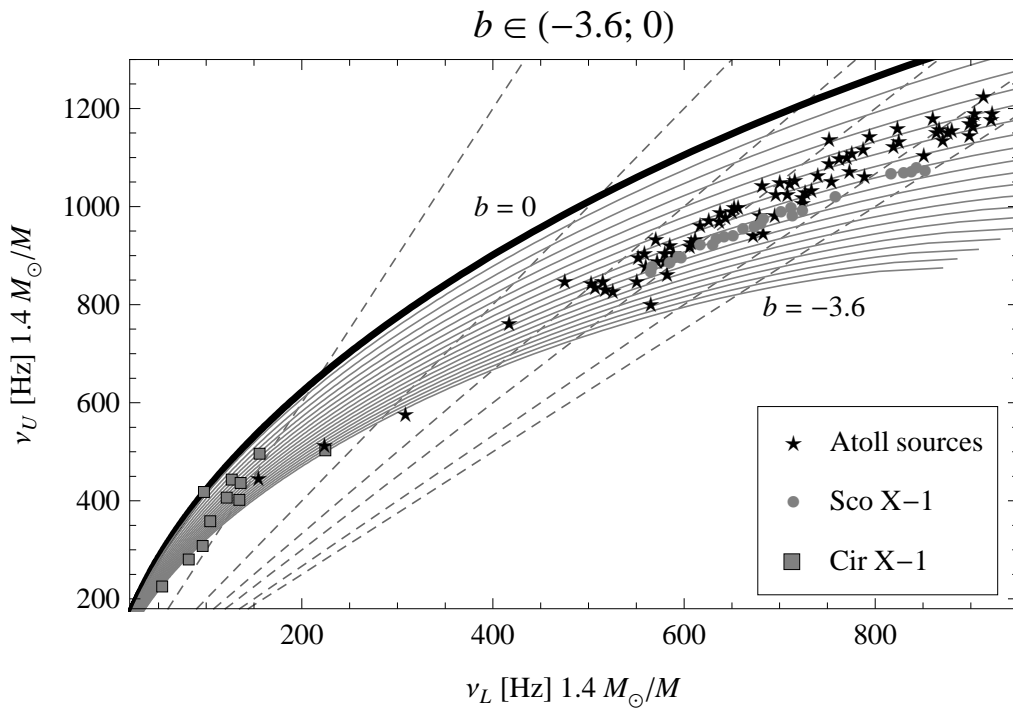
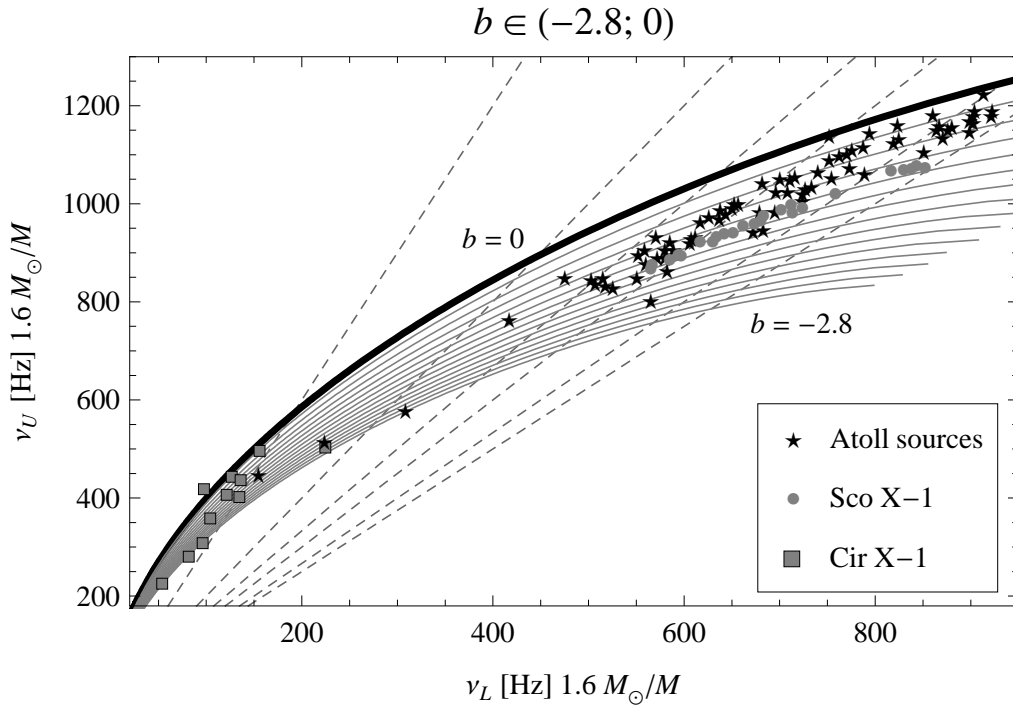


Figure 5. The relativistic precession model (with negative tidal charge) fits for atoll sources, Sco X-1 and Cir X-1 for various values of the brany parameter b ; the curves are spaced by 0.2 in b . The grey dashed lines represent the frequency ratios $\nu_U : \nu_L = 3:1, 2:1, 5:3, 3:2, 4:3$ and $5:4$ subsequently left to right.

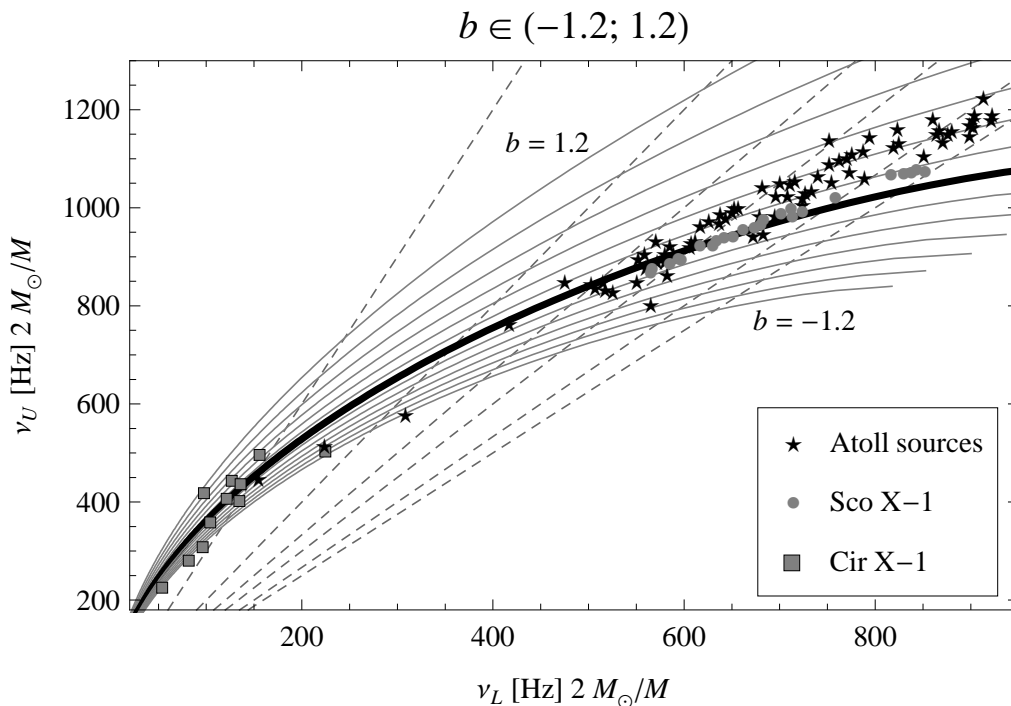


Figure 6. The relativistic precession model (with positive and negative tidal charge) fits for the same ensemble of data as in figure 5. Note that the $M = 2 M_{\odot}$, $b = 0$ RP frequency relation is commonly used for the fitting of observed QPO data (see, e.g., [25]).

The presented method is rough but robust, since the effects of neutron star rotation are not important. According to (41), the effect of the tidal charge is given by the term $\sim b/r^2$. On the other hand, the leading term giving rotational effects is $\sim a/r^{3/2}$ and, moreover, the limits on the rotational parameters taken from observed rotational frequencies of neutron stars [36] put a strong limit of $a \leq 0.3$, so that its influence onto the character of the fitting frequency-frequency curves is small as shown by Török et al. [36]. Of course, fitting the observational data of individual sources by precise methods will need the rotational parameter for fine tuning. ¶

Assuming negative values of B and positive values of λ , we obtained rough estimates $|B| < 1.5 \times 10^{11} \text{ cm}^2$ and $|\lambda| > 3 \times 10^{15} \text{ g/cm}^3$ for both $M \sim 1.6 M_{\odot}$ and the canonical case of neutron stars with $M \sim 1.4 M_{\odot}$. On the other hand, from the limits allowing both positive and negative values of b (λ), starting from the standard mass estimate $M \sim 2 M_{\odot}$ related to QPOs [24], we obtained a lower estimate of $|B| < 10^{11} \text{ cm}^2$, but higher values of $|\lambda| > 10^{16} \text{ g/cm}^3$.

These values should be confronted with estimates given by Böhmer et al. [12], concerning the effects of tidal charge in the limit of weak gravitational field related to

¶ The precise estimates of individual sources probably require also inclusion of the non-geodesic effects caused by the neutron star magnetic field [63].

the solar system. They considered the perihelion precession (Mercury), deflection of light near the edge of Sun, and the radar echo delay experiment. Clearly, the most convenient for comparison seems to be the first phenomenon, being of the same nature as the epicyclic motion of blobs in the relativistic precession model. The weak field restrictions are [12]

$$|B| < 5 \times 10^8 \text{ cm}^2, \quad \lambda > 7 \times 10^{13} \text{ g/cm}^3. \quad (71)$$

Note that the rough strong field regime model gives estimates of the tidal charge higher than the weak field regime in more than two orders of magnitude. However, as stressed in [12], a substantial part of the perihelion shift could correspond to the effect of solar oblateness, modifying thus, in principle, very strongly the estimates of B and λ . On the other hand, the restrictions implied in [12] by the light deflection and radar echo delay are $|B| < 10^{19} \text{ cm}^2$ and $|\lambda| > 10^{17} \text{ g/cm}^3$, which are substantially, by orders, higher than those given by rough estimates of QPOs observational data in X-ray binaries. We can thus conclude that the restrictions on $|B|$ and $|\lambda|$ implied by rough fitting of the neutron star X-ray binaries kHz QPOs data, i.e., in the strong gravitational field regime, give better fits as compared to those implied by the weak-field limit, if these results are not masked by the effects of the solar oblateness. Clearly, further and more detailed studies of all these phenomena are necessary. Moreover, there is a variety of other vacuum solutions of spherically symmetric static field on the brane [64, 65, 66] that deserve attention and have to be tested separately since the Weyl tensor in the complete 5D theory is unknown yet.

We plan to make further, more sophisticated comparisons of the plausible kHz QPOs models for neutron star X-ray binaries, including the RP model and the resonance disc oscillation ones, and compare these models with data obtained for individual sources. Precise fitting of these individual source data to the models including the influence of the tidal charge could, in principle, bring some new interesting results and limits on the tidal charge and brane tension although we cannot expect substantial shift of the rough estimates presented here, but rather better fits of observational data and more realistic estimates of the neutron star mass, more close to the expected canonical value. In fact, generally, we can conclude that the presence of a negative tidal charge enables lowering of the neutron star mass as can be seen from our rough estimates.

Acknowledgments

This work was supported by the Czech grant MSM 4781305903.

References

- [1] N. Arkani-Hamed, S. Dimopoulos, and G. Dvali. The Hierarchy Problem and New Dimensions at a Millimeter. *Phys. Lett. B*, 429:263–272, 1998. [arXiv:hep-ph/9803315v1](#).
- [2] L. Randall and R. Sundrum. An Alternative to Compactification. *Phys. Rev. Lett.*, 83(23):4690–4693, 1999. [arXiv:hep-th/9906064v1](#).

- [3] T. Shiromizu, K. i. Maeda, and M. Sasaki. The Einstein Equations on the 3-Brane World. *Phys. Rev. D*, 62:024012, 2000. [arXiv:gr-qc/9910076v3](#).
- [4] N. Dadhich, R. Maartens, P. Papadopoulos, and V. Rezania. Black holes on the brane. *Phys. Lett. B*, 487:1, 2000. [arXiv:hep-th/0003061v3](#).
- [5] C. Germani and R. Maartens. Stars in the braneworld. *Phys. Rev. D*, 64:124010, 2001. [arXiv:hep-th/0107011v3](#).
- [6] R. Maartens. Brane-world gravity. *Living Rev. Rel.*, 7:7, 2004. [arXiv:gr-qc/0312059v2](#).
- [7] C. W. Misner, K. S. Thorne, and J. A. Wheeler. *Gravitation*. W. H. Freeman and Co, New York, San Francisco, 1973.
- [8] M. Sasaki, T. Shiromizu, and K. i. Maeda. Gravity, stability, and energy conservation on the Randall–Sundrum brane world. *Phys. Rev. D*, 62:024008, 2000. [arXiv:hep-th/9912233v3](#).
- [9] A. N. Aliev and A. E. Gümrükçüoğlu. Charged rotating black holes on a 3-brane. *Phys. Rev. D*, 71(10):104027, 2005. [arXiv:hep-th/0502223v2](#).
- [10] F. Weber and N. K. Glendenning. Application of the improved Hartle method for the construction of general relativistic rotating neutron star models. *Astrophys. J.*, 390:541–549, 1992.
- [11] N. K. Glendenning. *Compact Stars: Nuclear Physics, Particle Physics, and General Relativity*. Springer-Verlag, New York, 1997.
- [12] C. G. Böhrmer, T. Harko, and F. S. N. Lobo. Solar system tests of brane world models. *Classical Quantum Gravity*, 25(4):5015, 2008. [arXiv:0801.1375v2 \[gr-qc\]](#).
- [13] J. Ponce de Leon. Static exteriors for nonstatic braneworld stars. *Classical Quantum Gravity*, 25:5012, 2008. [arXiv:0711.4415v2 \[gr-qc\]](#).
- [14] C. R. Keeton and A. O. Petters. Formalism for testing theories of gravity using lensing by compact objects. III. Braneworld gravity. *Phys. Rev. D*, 73(10):104032, 2006. [arXiv:gr-qc/0603061v3](#).
- [15] V. Bozza. Gravitational lensing in the strong field limit. *Phys. Rev. D*, 66(10):103001, 2002.
- [16] E. F. Eiroa. Braneworld black hole gravitational lens: Strong field limit analysis. *Phys. Rev. D*, 71(8):083010, 2005. [arXiv:gr-qc/0410128v2](#).
- [17] R. Whisker. Strong gravitational lensing by braneworld black holes. *Phys. Rev. D*, 71(6):064004, 2005. [arXiv:astro-ph/0411786v3](#).
- [18] J. Schee and Z. Stuchlík. Spectral line profile of radiating ring orbiting a brany Kerr black hole. In Hledík and Stuchlík [67], pages 209–220.
- [19] J. Schee and Z. Stuchlík. Optical effects in brany Kerr spacetimes. In Hledík and Stuchlík [67], pages 221–256.
- [20] R. A. Remillard and J. E. McClintock. X-Ray Properties of Black-Hole Binaries. *Annual Review of Astronomy and Astrophysics*, 44(1):49–92, September 2006. [arXiv:astro-ph/0606352v1](#).
- [21] M. van der Klis. Rapid X-ray Variability. In W. H. G. Lewin and M. van der Klis, editors, *Compact Stellar X-Ray Sources*, pages 39–112, Cambridge, 2006. Cambridge University Press.
- [22] M. van der Klis. Millisecond Oscillations in X-ray Binaries. *Annual Review of Astronomy and Astrophysics*, 38:717–760, 2000. [arXiv:astro-ph/0001167v1](#).
- [23] G. Török, M. A. Abramowicz, W. Kluźniak, and Z. Stuchlík. The orbital resonance model for twin peak kHz quasi periodic oscillations in microquasars. *Astronomy and Astrophysics*, 436(1):1–8, 2005.
- [24] T. Belloni, M. Méndez, and J. Homan. The distribution of kHz QPO frequencies in bright low mass X-ray binaries. *Astronomy and Astrophysics*, 437:209–216, 2005. [arXiv:astro-ph/0501186v2](#).
- [25] T. Belloni, M. Méndez, and J. Homan. On the kHz QPO frequency correlations in bright neutron star X-ray binaries. *Monthly Notices Roy. Astronom. Soc.*, 376:1133–1138, 2007. [arXiv:astro-ph/0702157v1](#).
- [26] D. Barret, J.-F. Olive, and M. Coleman Miller. An abrupt drop in the coherence of the lower kilohertz QPO in 4U 1636–536. *Monthly Notices Roy. Astronom. Soc.*, 361:855–860, 2005. [arXiv:astro-ph/0505402v1](#).
- [27] G. Török. Reverse of twin peak QPO amplitude relationship in six atoll sources. *Astronomy and Astrophysics*, submitted, 2008.

- [28] T. E. Strohmayer, R.F. Mushotzky, L. Winter, R. Soria, P. Uttley, and M. Cropper. Quasi-periodic Variability in NGC 5408 X-1. *Astrophys. J.*, 660:580–586, 2007. [arXiv:astro-ph/0701390v1](#).
- [29] P. Lachowicz, B. Czerny, and M. A. Abramowicz. Wavelet analysis of MCG-6-30-15 and NGC 4051: a possible discovery of QPOs in 2:1 and 3:2 resonance. *Monthly Notices Roy. Astronom. Soc.*, submitted, 2006. [arXiv:astro-ph/0607594v1](#).
- [30] B. Aschenbach, N. Grosso, D. Porquet, and P. Predehl. X-ray flares reveal mass and angular momentum of the Galactic Center black hole. *Astronomy and Astrophysics*, 417:71–78, 2004. [arXiv:astro-ph/0401589v2](#).
- [31] G. Török. A possible 3:2 orbital epicyclic resonance in QPOs frequencies of Sgr A*. *Astronomy and Astrophysics*, 440(1):1–4, 2005. [arXiv:astro-ph/0412500v1](#).
- [32] G. Török, M. A. Abramowicz, P. Bakala, M. Bursa, J. Horák, P. Rebusco, and Z. Stuchlík. On the origin of clustering of frequency ratios in the atoll source 4U 1636–53. *Acta Astronom.*, 58:113–119, 2008. [arXiv:0802.4026v2 \[astro-ph\]](#).
- [33] G. Török, M. A. Abramowicz, P. Bakala, M. Bursa, J. Horák, W. Kluźniak, P. Rebusco, and Z. Stuchlík. Distribution of kilohertz QPO frequencies and their ratios in the atoll source 4U 1636–53. *Acta Astronom.*, 58:15–21, 2008. [arXiv:0802.4070v2 \[astro-ph\]](#).
- [34] Z. Stuchlík and A. Kotrlová. Orbital resonances in discs around braneworld Kerr black holes. *General Relativity and Gravitation*, accepted, 2008.
- [35] L. Stella and M. Vietri. Lense–Thirring Precession and Quasi-periodic Oscillations in Low-Mass X-Ray Binaries. *Astrophys. J. Lett.*, 492:L59–L62, 1998. [arXiv:astro-ph/9709085v1](#).
- [36] G. Török, P. Bakala, Z. Stuchlík, and P. Čech. Modelling the twin peak QPO distribution in the atoll source 4U 1636–53. *Acta Astronom.*, 58:1–14, 2008.
- [37] G. Török, M. Bursa, J. Horák, Z. Stuchlík, and P. Bakala. On mutual relation of kHz QPOs. In Hledík and Stuchlík [67], pages 501–510.
- [38] S. Kato, J. Fukue, and S. Mineshige. Black-hole accretion disks. In Shoji Kato, Jun Fukue, and Sin Mineshige, editors, *Black-hole accretion disks*, Kyoto, Japan, 1998. Kyoto University Press.
- [39] W. Kluźniak and M. A. Abramowicz. The physics of kHz QPOs – strong gravity’s coupled anharmonic oscillators, 2001. [arXiv:astro-ph/0105057v1](#).
- [40] L. Rezzolla, S.i. Yoshida, T. J. Maccarone, and O. Zanotti. A new simple model for high-frequency quasi-periodic oscillations in black hole candidates. *Monthly Notices Roy. Astronom. Soc.*, 344(3):L37–L41, 2003. [arXiv:astro-ph/0307487v1](#).
- [41] G. Török and Z. Stuchlík. Epicyclic frequencies of Keplerian motion in Kerr spacetimes. In Hledík and Stuchlík [68], pages 315–338.
- [42] G. Török and Z. Stuchlík. Radial and vertical epicyclic frequencies of Keplerian motion in the field of Kerr naked singularities. Comparison with the black hole case and possible instability of naked singularity accretion discs. *Astronomy and Astrophysics*, 437(3):775–788, 2005. [arXiv:astro-ph/0502127v1](#).
- [43] Z. Stuchlík, A. Kotrlová, and G. Török. Multi-resonance models of QPOs. In Hledík and Stuchlík [67], pages 363–416.
- [44] E. Šrámková. Epicyclic oscillation modes of a Newtonian, non-slender torus. *Astronom. Nachr.*, 326(9):835–837, 2005.
- [45] O. M. Blaes, E. Šrámková, M. A. Abramowicz, W. Kluźniak, and U. Torkelsson. Epicyclic Oscillations of Fluid Bodies: Newtonian Nonslender Torus. *Astrophys. J.*, 665:642–653, 2007. [arXiv:0706.4483v1 \[astro-ph\]](#).
- [46] L. D. Landau and E. M. Lifshitz. *Mechanics*, volume I of *Course of Theoretical Physics*. Elsevier Butterworth-Heinemann, Oxford, 3rd edition, 1976.
- [47] A. H. Nayfeh and D. T. Mook. *Nonlinear Oscillations*. Wiley-interscience, New York, 1979.
- [48] M. A. Abramowicz, D. Barret, M. Bursa, J. Horák, W. Kluźniak, P. Rebusco, and G. Török. A note on the slope-shift anticorrelation in the neutron star kHz QPOs data. In Hledík and Stuchlík [68], pages 1–9.
- [49] M. A. Abramowicz, D. Barret, M. Bursa, J. Horák, W. Kluźniak, P. Rebusco, and G. Török.

- The correlations and anticorrelations in QPO data. *Astronom. Nachr.*, 326(9):864–866, 2005. [arXiv:astro-ph/0510462v1](#).
- [50] A. N. Aliev and D. V. Galtsov. Radiation from relativistic particles in nongeodesic motion in a strong gravitational field. *General Relativity and Gravitation*, 13:899–912, 1981.
- [51] M. Jaroszyński, M. A. Abramowicz, and B. Paczyński. Supercritical accretion disks around black holes. *Acta Astronom.*, 30:1–34, 1980.
- [52] B. Paczyński and P. J. Wiita. Thick accretion disks and supercritical luminosities. *Astronomy and Astrophysics*, 88(1–2):23–31, 1980.
- [53] M. Kozłowski, M. Jaroszyński, and M. A. Abramowicz. The analytic theory of fluid disks orbiting the Kerr black hole. *Astronomy and Astrophysics*, 63(1–2):209–220, 1978.
- [54] J. H. Krolik and J. F. Hawley. Where Is the Inner Edge of an Accretion Disk around a Black Hole? *Astrophys. J.*, 573(2):754–763, 2002. [arXiv:astro-ph/0203289v1](#).
- [55] D. Barret, J.-F. Olive, and M. C. Miller. Drop of coherence of the lower kilo-Hz QPO in neutron stars: Is there a link with the innermost stable circular orbit? *Astronom. Nachr.*, 326:808–811, 2005. [arXiv:astro-ph/0510094v1](#).
- [56] D. Barret, J.-F. Olive, and M. C. Miller. The coherence of kilohertz quasi-periodic oscillations in the X-rays from accreting neutron stars. *Monthly Notices Roy. Astronom. Soc.*, 370:1140–1146, 2006. [arXiv:astro-ph/0605486v1](#).
- [57] G. Török, Z. Stuchlík, and P. Bakala. A remark about possible unity of the neutron star and black hole high frequency QPOs. *Central European J. Phys.*, 5(4):457–462, 2007.
- [58] Z. Stuchlík, G. Török, and P. Bakala. On a multi-resonant origin of high frequency quasiperiodic oscillations in the neutron-star X-ray binary 4U 1636–53. *Astronomy and Astrophysics*, submitted, 2007. [arXiv:0704.2318v2 \[astro-ph\]](#).
- [59] M. A. Abramowicz, T. Bulik, M. Bursa, and W. Kluźniak. Evidence for a 2:3 resonance in Sco X-1 kHz QPOs. *Astronomy and Astrophysics*, 404:L21–L24, 2003. [arXiv:astro-ph/0206490v2](#).
- [60] S. Boutloukos, M. van der Klis, D. Altamirano, M. Klein-Wolt, R. Wijnands, P. G. Jonker, and R. P. Fender. Discovery of Twin kHz QPOs in the Peculiar X-Ray Binary Circinus X-1. *Astrophys. J.*, 653:1435–1444, 2006. [arXiv:astro-ph/0608089v2](#).
- [61] M. A. Abramowicz and W. Kluźniak. A precise determination of black hole spin in GRO J1655–40. *Astronomy and Astrophysics*, 374:L19, 2001. [arXiv:astro-ph/0105077v1](#).
- [62] W. Kluźniak and M. A. Abramowicz. Strong-field gravity and orbital resonance in black holes and neutron stars – kHz quasi-periodic oscillations (QPO). *Acta Phys. Polon. B*, 32:3605–3612, 2001.
- [63] P. Bakala, E. Šrámková, Z. Stuchlík, and G. Török. On magnetic-field induced non-geodesic corrections to the relativistic precession QPO model. *Astrophys. J.*, submitted, 2008.
- [64] S. Shankaranarayanan and N. Dadhich. Non-Singular Black-Holes on the Brane. *Int. J. Modern Phys. D*, 13:1095–1103, 2004. [arXiv:gr-qc/0306111v2](#).
- [65] R. Casadio and L. Mazzacurati. Bulk Shape of Brane-World Black Holes. *Modern Phys. Lett. A*, 18:651–660, 2003. [arXiv:gr-qc/0205129v2](#).
- [66] R. Casadio, A. Fabbri, and L. Mazzacurati. New black holes in the brane world? *Phys. Rev. D*, 65(8):084040, 2002. [arXiv:gr-qc/0111072v2](#).
- [67] S. Hledík and Z. Stuchlík, editors. *Proceedings of RAGtime 8/9: Workshops on black holes and neutron stars, Opava, Hradec nad Moravicí, 15–19/19–21 September 2006/2007*, Opava, 2007. Silesian University in Opava.
- [68] S. Hledík and Z. Stuchlík, editors. *Proceedings of RAGtime 6/7: Workshops on black holes and neutron stars, Opava, 16–18/18–20 September 2004/2005*, Opava, 2005. Silesian University in Opava.